International Conference on Space Optics—ICSO 2022

Dubrovnik, Croatia

3–7 October 2022

Edited by Kyriaki Minoglou, Nikos Karafolas, and Bruno Cugny,

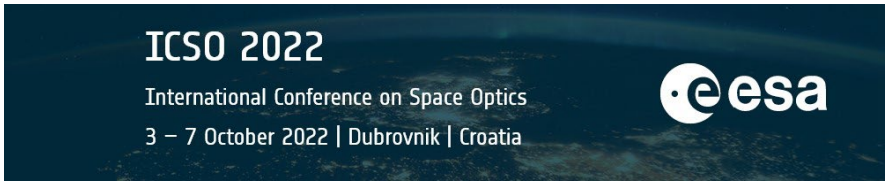

HgCdTe APD detector module for deep space optical communications

International Conference on Space Optics — ICSO 2022, edited by Kyriaki Minoglou, Nikos Karafolas, Bruno Cugny, Proc. of SPIE Vol. 12777, 127774B · © 2023 ESA and CNES · 0277-786X · doi: 10.1117/12.2690826

HgCdTe APD detector module for deep space optical communications

J. Rothman*[a], S. Pes[a], J. Abergel[a], S. Gout[a], A. Coquiard[a], G. Badano[a], G. Lasfargues[a], A. Vandeneyde[a], J.-A. Nicolas[a], J.-L. Santailler[a], S. Mejri[b]
[a]Univ. Grenoble Alpes, CEA,/Leti, 17 rue des Martyrs F-38054 Grenoble, France,
[b]ESA/ESOC, Robert-Bosch-Str. 5, D-64293 Darmstadt, Germany

ABSTRACT

A 4-quadrant large area HgCdTe APD detector module have been developed and characterized in view of application in deep space optical communications. Single photon detection capacity has been demonstrated on each of the four channels of the detector module, associated with a bandwidth close to 400 MHz. The performance for pulse position modulation (ppm) has been estimated from the detection of strongly attenuated laser pulses and were found to be close to the system performance specifications given by ESA: the pulse detection probability in a time slot of 800 ps was measured to be higher about 90 % for a signal of 7 photons focused on the center on one channels, associated with a false alarm rate below 1 %, although the sensitivity of the full detector module was limited by a low quantum efficiency and a high dark count rate. With a 16-ary ppm modulation, this corresponds to a data rate of 320 Mbps at less than 2 photons per bit.

Keywords: HgCdTe, APD, free space optical communications, deep space, photon counting

1. INTRODUCTION

HgCdTe APDs enables linear detection of low number of photons, down to single photons, at high rate due their intrinsically high quantum efficiency, high linear avalanche gain, low excess noise and low impact of the APD gain on their temporal response [1]. These characteristics allows to increase sensitivity, speed and/or linearity that are of interest in applications such as free space optical communications, lidar and quantum optical information processing [2]-[4].

The use of HgCdTe APD detector for deep space optical communications was first demonstrated within the scope of NASAs Lunar Laser Communication Demonstration (LLCD), in which a detector from CEA/Leti was used to receive up to 78 Mbps at 20 photons per bit 16-ary pulse position modulated (ppm) data at ESAs OGS on Tenerife [5],[6]. A higher data-rate (622 Mbps) at a lower value of ppb was demonstrated by NASA and MIT/LL using super conduction nano-wire detectors (SNSPDs) [7]. The difference in performance between the two demonstration can be related to the dedicated development and optimization to the SNSPDs based receiver system, whereas the HgCdTe APD was assembled using an APD originally developed for Lidar applications. These two detector technologies singles out as the two most promising technologies for down to single photon applications such as deep space communication and quantum information processing. Their present advantages and limitations are compared in Table 1. The difference in performance imply that HgCdTe APD based detector enables a higher data, a higher dynamic range and a reduced sensitivity to saturation due to background radiation. SNSPDs presents an advantage in very high order ppm in which the intrinsic detector dark count rate need to be very low to obtain a low false alarm rate. This short analysis indicates that HgCdTe APDs are expected to present an advantage for moderate deep space applications whereas SNSPDs detectors could be preferable in communications from the largest distances and at low data rates.

Table 1. Comparison of typical advantages and limitations of SNSPDs and HgCdTe APDs.

Technology	Advantages	Limitaions
SNSPDs	- High detection efficiency : 90 % - Low dark count rate : < 1 kHz - Low jitter : < 100 ps	- Low operating temperature : < 4K - Long recovery time : > 10 ns (implies a limited detection rate and dynamic range)
HgCdTe APDs	- High bandwidth and data rates : > 500 MHz - Low jitter with optimized optical coupling <100 ps - High dynamic range : > 60 dB - Relatively high operating temperature :> 80 K	- Moderate detection efficiency : > 50 % - High dark noise and dark count rate : > 500 kHz (potentially limitated by glow from Si CMOS amplifier)

*johan.rothman@cea.fr

In this communication, we report on the results from the first dedicated development and characterization of a free space optical coupled 4-channel HgCdTe APD detection module for high data rate deep space optical communications with close to a single photon per bit. The detection module has been designed to respond to ESAs objectives to dispose of a large area 4-quadrant detector with single photon detection capacity. The system specifications of the detection module are resumed in Table 2. The 4-quadrant configuration allows to use the detector both for data detection and beam steering, with the goal to simplify the optical system and increase the number of photons on the detector. First characterization of single element APDs made during the development of this module using APDs with a small optical area. These measurements have shown that the detectors enables down to single photon detection with a high quantum efficiency and low excess noise at a record high detection rate, in excess of 500 MHz, and with a dark count rate of 500 kHz. These results shows on the strong potential of this technology to detect and process information at a single photon signal level [4],[8].

The results from the characterization of the fully functional large area 4-quadrant HgCdTe APD detection module. The detector design and the experimental procedures are detailed in section 2 and 3. The characterization results are reported in section 4. Section 5 presents a general conclusion of the presented results and perspectives for the development of HgCdTe APD base detector modules for deep space optical communications.

Table 2. System performance specifications for the detector module.

System performance parameter	ESA specification
a)Overall size	400 x400 µm (4 quadrants of 200x200 µm)
b)Gap between quadrants	To be minimized
c)Wavelength range	1000 - 1600 nm
d)Minimum signal per pulse	5 photons (goal: 1 photon)
e)Pulse width (PPM slot width)	ranging from 0.5 (goal: 0.2) to 500 ns
f)Minimum slot separation	one “empty” slot
g)Response time jitter	100 ps
h)Minimum dynamic range	20 dB (goal 30 dB)
i)Detection probability	0.9 (goal: 0.99) tbc
j)False alarm probability	10^{-2} (goal: 10^{-3}) tbc

2. DETECTION MODULE DEVELOPMENT

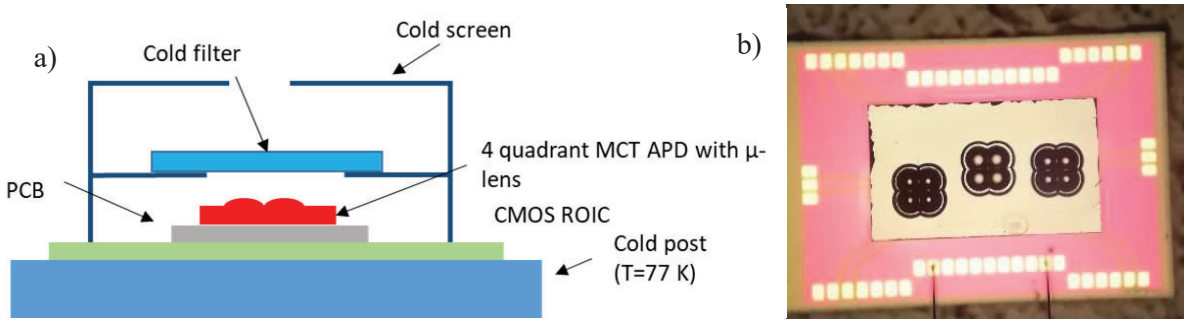

Figure 1. a) Schematic of the detector module components inside the LN2 cryostat and b) micro-graph of 4-quadrant micro-lenses made into an HgCdTe APD die.

HgCdTe APDs offers a unique opportunity to respond to the requirements for high rate deep space optical communication at close to a single photon level thanks to the possibility to combine high gain, fast response time without dead-time and low dark current at relatively high operating temperature, in particular compared to SNSPDs. The high operating temperature is a main advantage to enable an operation of a detector using free space optical coupling with the detector directly mounted on the receiver telescope, which is required to take advantage of the 4-quadrant configuration. The high bandwidth and absence of dead time do also constitute advantages in view of increasing the data rate, using reduced slot-widths, and to avoid saturation of the detector from stray light.

Nevertheless, the development of such a detector that responds to the requirement specified by ESA for deep space optical communications using HgCdTe APDs represents multiple challenges that have been addressed by the development and assembly of several sub-components, illustrated in Figure 1.

To enable single photon detection in HgCdTe APDs, the APDs needs to be hybridized directly onto a specifically designed Si-CMOS amplifier. This allows to obtain a maximum bandwidth at minimal noise through the reduction of the input capacitance of the amplifier, for example through the suppression of bond-pads. A specifically designed resistive feed-back trans-impedance amplifier (RTIA) with 4 channels, termed CL110, was designed and procured at CEA/Leti with this objective. The first characterization of this amplifier have shown that this approach have enabled a bandwidth in excess of 400 MHz combined with an input noise of 40 electrons and have enabled single photon detection at an APD gain of about 200 [4],[8]. As a comparison, the input noise of a deported RTIA amplifier is typically in excess 300 electrons and would require an APD gain of 1000 to reach single photon detection capacity.

Each channel of the amplifier have an individual differential output that is buffered to drive 50 Ohms impedances. The four channels are referred to as C12, C34, C56 and C78.

The use of a hybridized amplifier do however imply that the APD capacitance and junction area need to be small in order to preserve the performance of the amplifier. In the case of CL110, this implies that the diameter of the APDs needs to be small, typically below 20-30 µm, depending on the multiplication layer width. This is an order of magnitude below ESAs requirement for the optical active are (see Table 2). A solution to this problem is to implement micro-lenses that are monolithically integrated into the substrate. This capacity was recently developed at CEA/Leti [3] and allows forming close to diffraction limited lenses that image the field of view of the detector onto the APD, when the latter is placed at the focus of the micro-lens. In the present detector design, a focal distance of 400 µm was implemented onto the detector demonstrator that allows to form a 15 µm diameter spot on the APD with an F/10 focusing optics [3]. This focal distance was selected as a compromise between the spot size, that is increase with the focal distance, and the topology of the lens, that is reduced with the focal distance in favor of a better control of the shaping of the micro lenses. Typical 4-quadrant lenses made with a nominal focal distance of 400 µm are illustrated in Figure 1 b). The shaping of such lens is more problematic than for a single lens, in particular at the intersection of the lenses, and its impact on the optical coupling onto the different channels are discussed in section 4.

In order to obtain a fast response for all detected photons, the signal for each channel needs to be focused within the active area of the APDs to avoid a slow diffusion collection of carriers that will generate temporal jitter and, as a consequence, limitations in the minimal slot width that can be achieved with the detector. A dedicated batch have been processed with four HgCdTe wafers to form APD dies compatible with the 200 µm pitch 4-quadrant configuration implemented on the CL110. APD dies were made with different diameters, with the objective to select the geometry with the best compromise in terms of optical coupling to the APD, optimized with a large area APD, and amplifier performance, which is optimal for APDs with a small diameter. These APDs were processed with a technology that was initially developed for focal plane array application with a diode diameter below 10 µm. However, this technology have been found to be incompatible with the formation of large diameter APDs with fast response and high gain, which is why we could only use a 10 µm diameter APDs in the present detector module that is expected to limit the detection efficiency and temporal resolution of the detector. This technological limitation has spurred the successful development of a new APDs process that have been shown to enable the a fast response, BW close to 2 GHz, at high APD gains, in excess of 100, in APDs with a diameter up to 40 µm [9]. The hybridization of such APDs onto the CL110 offers a high potential to optimize the performance of HgCdTe APDs for photons counting applications that is further discussed in section 5.

The hybridized detector module is mounted onto a PCB that has been designed to stabilize the bias supplies to the detector and to optimize the thermal coupling of the hybrid detector with the cold post. A cold screen (open at F/8) and a cold low pass optical filter (cut-off at 2.5 µm) have been implemented onto the PCB with the goal to minimize the stray-light on the detector and the resulting dark noise.

3. EXPERIMENTAL PROCEDURES

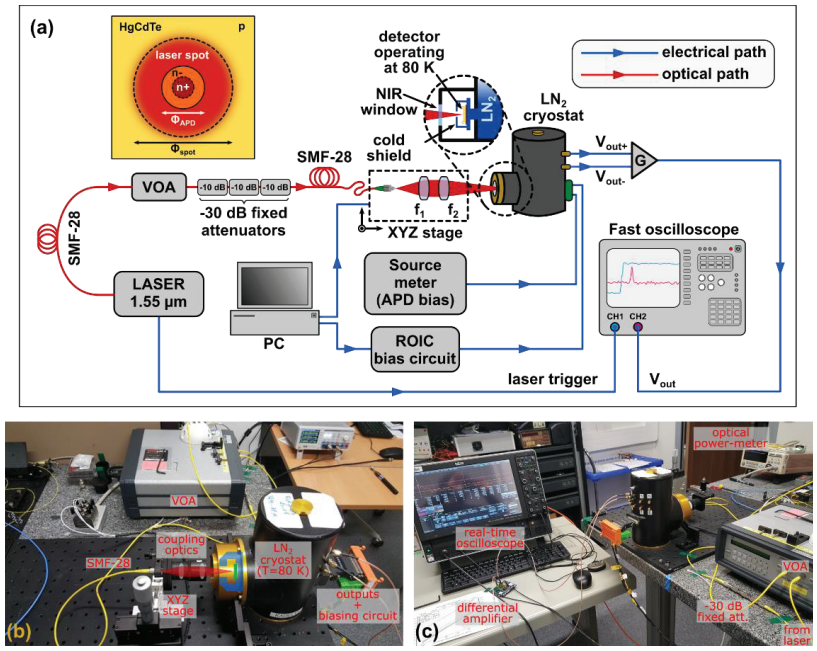

Figure 2. Experimental setup that is used to perform basic characterization of the detection modules: (a) schematics and (b,c) photos of the bench.

The module has been characterized using the experimental setup depicted in Figure 2. A gain switched laser source (Calmar Optcom) emitting at λ_{laser} = 1550 nm has been used to generate laser pulses with a pulse width of ~ 40 ps and at a repetition rate frate whose value could be set in a range between 1 MHz and 1 GHz (f_{rate} = 4 MHz was set during the measurements, if not otherwise specified). The laser output was then coupled on a single-mode fiber (SMF-28). The jitter of the laser pulses is negligible compared to that of the detector and equal to ~1 ps (as declared by the laser supplier). The average power of the optical signal sent to the detector was controlled by means of a variable optical attenuator (VOA), which allowed a real-time monitoring of the input power thanks to an integrated power meter. A cascade of three 10 dB fixed optical attenuators (30 dB of attenuation in total) was added after the VOA, in order to reach the single photon level before sending the light on the detector surface.

The setup has been calibrated using a high sensitive optical power meter (Keysight 8163B) at the end of the fiber. This allowed estimating the optical losses due to fiber connectors, which were taken into account to calculate the exact average number μ of photons per pulse of the Poissonian light at the input of the focusing optics.

The optical signal is then focused on the detector using a 2-lens optical system composed by a collimator with focal length f_1 = 37 mm and an achromatic lens with f_2 = 100 mm, which produces a laser spot of Φspot = 28 µm in diameter at its waist. Hence, this spot size is larger than the APD diameter, which is why a well optimized micro lens is needed in order to minimize the loss due the optical coupling. The expected spot size is 15 µm, which is larger than the presently available APD with a diameter of 10 µm and will reduce the quantum efficiency and increase the response time and jitter of the detector. The optical system has been mounted on a motorized xyz-stage that allows to map the response of each channel of the detector.

Finally, in order to estimate the performance of the detector with two consecutive pulses, a double pulse signal with a pulse separation δt between the pulses was generated using 2x2 optical couplers and an optical delay line, as illustrated in Figure 3.

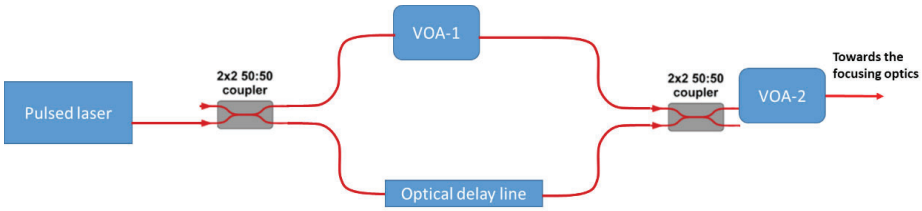

Figure 3. Modified set-up to form a double pulse width an equal amplitude and with an adjustable delay ΔT=0-2 ns

4. CHARACTERIZATION RESULTS

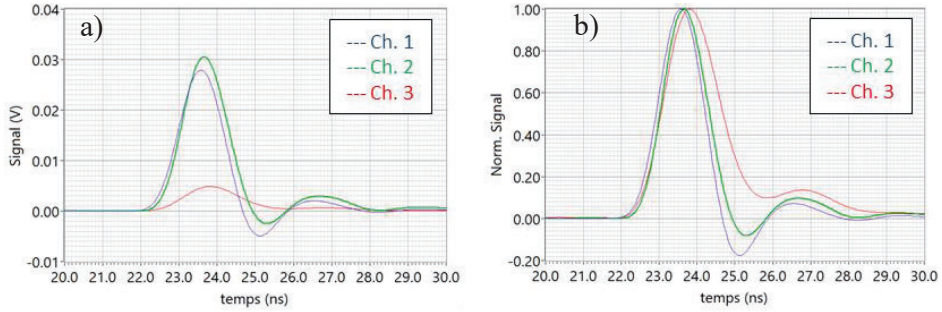

Figure 4. Raw (a) and Normalized (b) impulse response measured at unity gain on the channels C12, C34 and C56.

Table 3. Detector demonstrator characteristics measured at unity APD gain. The noise of the channel C56 has been estimated by subtracting the noise of the chain of detection (dominated by the differential amplifier)

CH	V_bias (V)	Popt (dBm)	Nph	QE (%)	Signal (mV)	noise (mV)	FWHM (ns)	G_RTIA (mV/photons)	Noise (photons)
12	0	-60.89	1589.2	50	27.95	1.51	1.37	0.0176	85.86
34	0	-60.89	1589.2	50	30.7	2.08	1.37	0.0193	107.67
56	0	-60.89	1589.2	50	4.7	0.27	1.65	0.0030	91.58
78	0	-60.89	1589.2	50	17.89	1.098	1.31	0.0113	97.54

All four channel were found to respond to light with a close to constant signal to noise ratio although the signal was found to vary between the channels. This variation in response at unity gain for three of the channels is illustrated in Figure 4. The unity gain performance of the detector module channels are resumed in Table 1. The origin of these variations has not yet been determined but they are consistent with an attenuation of the signal and noise due to the presence of an impedance on the output of the channels with a smaller response. The input referred noise level in photons, estimated by the ratio of the voltage noise and the fast signal amplitude response of the detector, is close to NEPh~100 photons on each channel. This value is higher than the one observed in the previously characterized devices, NEPh~60 photons [8]. The increase noise can be explained by use of different optical coupling in the previously reported measurement, in which the light was focused onto the detector using a lens with a smaller focal distance and without the use of a micro-lens. This results in a smaller spot size, in favor of a larger fraction of photons that contributes to the fast response and to a higher quantum efficiency. This conclusion is corroborated by the observation of a slightly wider pulse width in the present devise, FWHM=1.3 to 1.6 ns, compared to 1.2 ns observed on the previous devices. The deterioration in optical coupling will directly impact on the system performance of the present but it do also identify and quantify ways to optimize the detector the performance through the optimization of the optical coupling.

The characterization of the spatial response of the channels is reported in Figure 4. It can be seen that a response over 200 µm is obtained for all quadrants onto the small 10 µm diameter APD. The gap of low response is about 20 µm between adjacent channels. However, fluctuations in signal amplitude are observed within the detection area of each quadrant. These fluctuation were found to be correlated with an increased pulse width and a delayed detection. This indicates that they corresponds to a displacement and/or enlargement of the optical spot around the active area APD that is due to imperfection of the micro-lenses that varies between each quadrant. Nevertheless, this result constitute a first proof of principle of the use of such device and show that this approach represents a viable solution for deep space applications. It do also indicate that the detector can be operated in the nominal four a single channel mode although a single channel mode is preferable to achieve the highest sensitivity. The measured limitations of the optical coupling are

due to the use of a too small active APD diameter of 10 µm. These limitations are expected to be overcome in future devices using larger diameter APDs that were recently developed at CEA/Leti [9], and through an optimization of the lens design and processing.

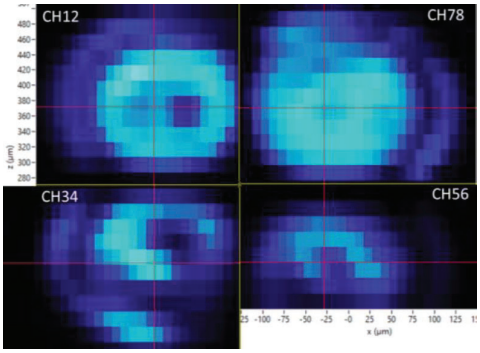

Figure 5. Mapping of the impulse response amplitude over the four channels of the demonstrator detector.

In order to achieve single photon detection capacity, the reverse bias needs to be increased to achieve a gain in excess of 100, given the high noise of the detector. Variation of the gain and the input photon noise for the four channels of the detector are reported in Figure 6. It can be seen that a gain in excess of 100 is observed on all channels and do allow the observation of single photon events on all channels. The imperfect optical coupling of the present device implies that this detection is made with a high jitter and loss due to large fraction of light that is absorbed outside the active APD area. The equivalent input noise reduces with the increased gain up to a reverse bias of about 10V. At higher reverse bias and gain, it can be seen that the reduction in noise saturates, in particular on channels C12 and C78. This saturation is due to the observation of dark events that contributes to the dark noise of the detector. These events can be due to stray light that leaks into the cryostat and/or to defect related generation within the APD. These events will increase the false alarm rate and limit the use of the detector for higher order ppm modulation schemes.

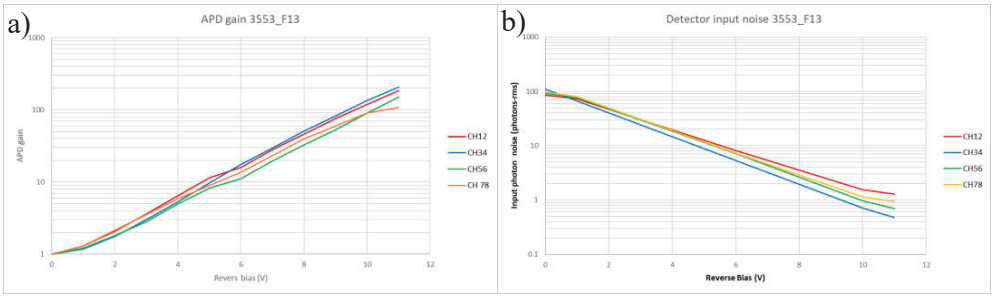

Figure 6. a) APD gain and b) equivalent input photons noise (NEPh) as a function reverse bias of the detector.

The performance of the detector module have been estimated for the system performance parameters given in Table 2 by fitting the observed pulses with a Gaussian function to estimate the amplitude and instant of detection of each pulse, as detailed in [8]. The resulting data show that the observed performance is slightly below the requirements in terms of sensitivity and temporal resolution. The detection efficiency and false alarm for the channel C34 are illustrated in Figure 5 at 10, 5 and 1 photons per pulse (ppp). The false alarm rate displays a trailing bump which is due to the detection of dark events that implies the use of a high threshold amplitude of 15 mV to reach a false alarm rate of 10^{-2} . This threshold level corresponds to detection efficiencies of 98 %, 85 % and 20 % for 10, 5 and 1 ppp, respectively. Hence, the objectives in detection efficiency (90 %) and false alarm rate (10^{-2}) are met for a signal level between 5 and 10 ppp and can estimated to be close to 7 ppp. The supersession of the dark events, for example through the optimization of the cold screen and cold filter, allows reducing the threshold to about 5 mV which would allow reaching a the detection efficiency of 90 % at 5 ppp, in compliance with ESAs specification. In addition, an optimization of the optical coupling should enable to reduce the input signal with close a factor 2, neglecting the influence of the increased photon shot noise.

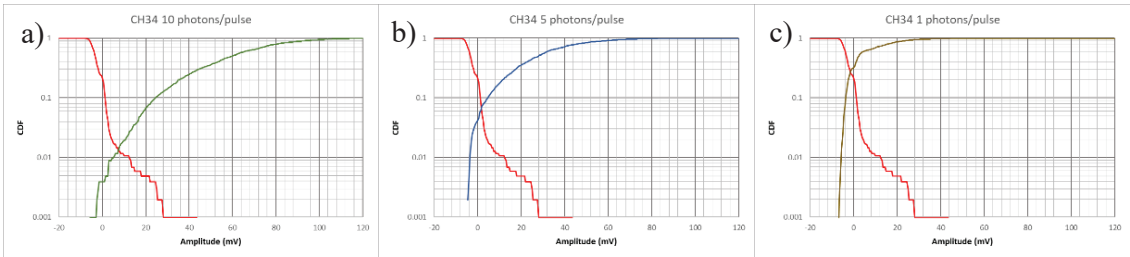

Figure 7. Cumulative and complementary cumulative distribution functions for the signal (CDF) and dark noise (CCDF) measured with a) 10 and b) 5 and c) 1 photons per pulse centered on channel C34 at a reverse bias of 11 V.

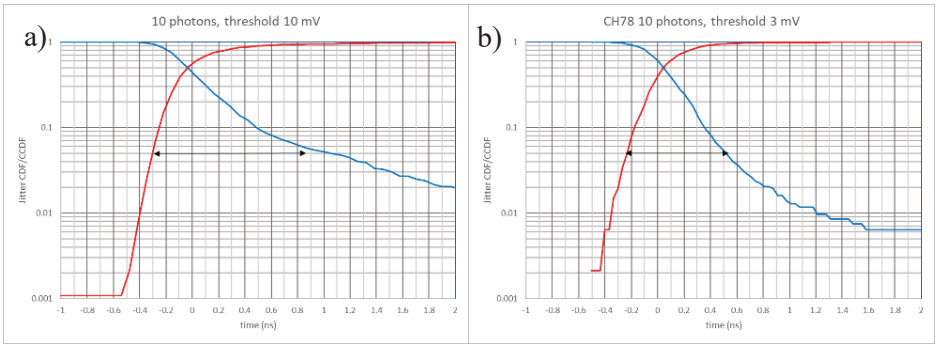

Figure 8. Cumulated and complementary cumulated distribution of the jitter on cannels a) C34 and b) C78.

The minimum slot width depends directly on the jitter of the instant of detection of the detector. The jitter was found to be FWHM=250 ps, which is higher than ESAs specification and the value that was reported in [8]. Again, this is due to the use of non-optimal coupling onto a too small APD. The cumulated distribution functions of the pulse position are reported in Figure 6 for two of the detector channels (C34 and C78). It can be seen that a slot width of down to 0.8 ns (with a probability of 90 % to detect the pulse in the good slot) is obtained on the channel (C78). The other channel (C34) needs to be operated with a slot width higher than 1 ns. The difference in required widths is likely to be due to a difference in optical coupling that generates a stronger delay in the charge collection on the channel C34.

The capacity of the detector to correctly detect two consecutive pulses with one empty slot was investigated with a slot width of 0.8 ns and a pulse separation of 1.6 ns, in consistency with the minimal slot width estimated above. In order to determine the pulse position of each impulse, the recorded signals were fitted with a double Gaussian fit with variable instant of arrival and amplitude for each impulse. Figure 9 shows the results of the fitting of three recordings with 10 photons in each pulse. The cumulative distribution functions of the pulse position of each pulse for channel C34 and C78 are shown in Figure 10. It can bee seen that the trailing edge from the first pulse tends to increase the width of the distribution of the second pulse. This is probably due to a contribution from photons that are absorbed far from the active area of the APD who generates events that are detected with a stronger delay. This behavior reduces the detection efficiency within the good slot even of C78, which is observed to be slightly lower than 90% in this case. Once again, this limitation can be addressed by using the new larger area APD technology [9] in order to optimize the optical coupling.

These results can be used to estimated the required number of photons per bit for a given modulation scheme. The minim slot width of 0.8 ns corresponds to 312 Mbps using a 16-ary ppm signal. This data rate can be detected with a detection efficiency of 0.9, a false alarm rate below 10^{-2} and less than 2 photons per bit when all light is concentrated on a single channel.

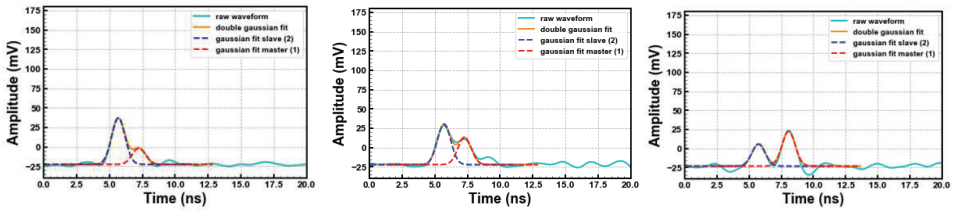

Figure 9. Comparison of the result of the double Gaussian adjustment on signals measured on CH34. The temporal window for the fitting of each signal was 12 ns, centered on the expected time of arrival.

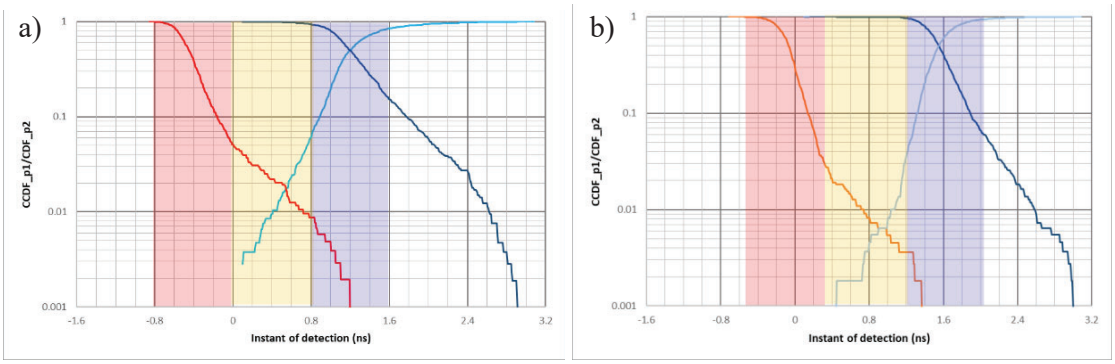

Figure 10. Complementary cumulative distributions for the instant of detection (pulse position) for the channels a) C34 and b) C78. The red squares indicates the position of the first slot (red), empty slot (yellow) and second slot (blue).

5. CONCLUSIONS AND PERSPECTIVES

A photon counting capable 4-quadrant detection module with large 200 µm diameter optical collection area for each quadrant have been developed for use in deep space optical communications and will be delivered to ESA in fall 2022. The detector have been characterized with the goal to evaluate the performance of the detector with respect to the system requirements for deep space optical communications using ppm modulation. The corresponding results are compared with the specification in Table 4. It can be seen that most of the parameters are compliant or close to compliant with the requirements although the detector was flawed by an imperfect optical coupling, due to the use of an APD with a too small diameter, and due to the presence of a high dark count rate. The perfectible optical coupling has a direct impact on both the sensitivity and the temporal resolution of the detector. The high dark count rate implies the need to use a high threshold level to reach the required false alarm rate, that reduces the detection efficiency at given signal level. This impact will be enhanced if the detector is used with high order ppm data that might be required for the deepest space application.

With the present limitation, the results shows on a capacity of the developed detector module to detect 16-order ppm at a slot width of about 0.8 ns, corresponding to 312 Mbps, with a detection efficiency of 0.9, false alarm rate below 10^{-2} and less than 2 photons per bit when all light is concentrated on a single channel. The performance of the detector can be strongly improved using a recently developed APD technology that allows forming APDs with large diameters, in favor of an optimized optical coupling, characterized by a high gain at bandwidths close to 2 GHz [9]. Such detectors, combined with a reduction of the dark count rate through an optimization of the cold screen of the detector, should enable the use this technology in the most demanding deep space optical communications. In addition, the association of such APDs with a higher bandwidth amplifier will enable to use such detectors at close to a single photon per bit at data rates up to 2 Gbps.

Table 4. Compliance table of the system performance of the final detector module.

System performance parameter	ESA technical specification	CEA deliverable
a)Overall size	400 x400 µm (4 quadrants of 200x200 µm)	**Compliant** with mirco-lens
b)Gap between quadrants	To be minimized	**20 µm gap** between the edges of the channels
c)Wavelength range	1000 - 1600 nm	**Compliant :** QE= 50 % measured at 1.55 µm
d)Minimum signal per pulse	5 photons (goal: 1 photon)	**Non-compliant** on a single channel (7 photons or higher APD gain is needed)
e)Pulse width (PPM slot width)	ranging from 0.5 (goal: 0.2) to 500 ns	**Non-compliant** : 0.8 ns at 0.9 detection probability in the correct slot on the best channel
f)Minimum slot separation	one "empty" slot	**~Compliant** at a slot width of 0.8 ns on the best channel
g)Response time jitter	100 ps	**Non-compliant** (FWHM =250 ps)
h)Minimum dynamic range	20 dB (goal 30 dB)	**Compliant** when distributed over all channels (require an optimized optical coupling)
i)Detection probability	0.9 (goal: 0.99) tbc	**~Compliant** (on a single channel for 7 photons)
j)False alarm probability	10^{-2} (goal: 10^{-3}) tbc	**~Compliant** (on a single channel for 7 photons)

ACKNOWLEDGEMENTS

The authors wish to acknowledge ESA for supporting this development under the ESA Technology and Research Program (TRP). The characterization of the photon counting modules has also been supported by the labex FOCUS.

REFERENCES

[1] Rothman, J., "Physics and Limitations of HgCdTe APDs: A Review," J. Electron. Mater. 47, 5657–5665 (2018)
[2] Rothman, J., Bleuet, P., Andre, L., Abadie, Q., Bordot, G., Bisotto, S., Audoit, G., Nicolas, J.-A., Dupont, B., Rostand, J.-P., and Lasfargues, G., "HgCdTe APDs for free space optical communications," Proc. SPIE 10524, 1052411 (2018)
[3] Rothman, J., Bleuet, P., Abergel, J., Gout, S., Lasfargues, G., Mathieu, L., Nicolas, J.-A., Rostaing, J.-P., Huet, S., Castelein, P., Aubaret, K., Saint-Pé, O., "HgCdTe APDs detector developments at CEA/Leti for atmospheric lidar and free space optical communications," Proc. SPIE 11180, 2018 International Conference on Space Optics (ICSO 2018), 111803S (2019)
[4] Rothman, J., Pes, S., Bleuet, P., Abergel, J., Gout, S., Nicolas, J.-A., Rostaing, J.-P., Renet, S., Mathieu L., and Le Perchec, J., "Meso-photonic detection with HgCdTe APDs at high count rates," J. Electron. Mater. 49, 6881–6892 (2020)
[5] Zayer, I., Sodnik, Z., Daddato, R.,J., Lanucara, M., Schulz, K.-J., Smit, H., Sans, M., Becker, P., Giggenbach, D., Mata-Calvo, R., Fuchs C., and Rothman, J., "Lunar Optical Communications Link Demonstration Between NASA's Ladee Spacecraft and ESA's Optical Ground Station," SpaceOps 2014 Conference, AIAA 2014-1919, (2014)
[6] J. Rothman, E. de Broniol, K. Foubert, L. Mollard, N. Péré-Laperne, F. Salvetti, A. Kerlain, and Y. Reibel "HgCdTe APDS for space applications", Proc. SPIE 10563, International Conference on Space Optics — ICSO 2014, 105631T (2017)
[7] Don M. Boroson, Bryan S. Robinson, Daniel V. Murphy, Dennis A. Burianek, Farzana Khatri, Joseph M. Kovalik, Zoran Sodnik, and Donald M. Cornwell "Overview and results of the Lunar Laser Communication Demonstration", Proc. SPIE 8971, Free-Space Laser Communication and Atmospheric Propagation XXVI, 89710S (2014)
[8] S. Pes, J. Rothman, P. Bleuet, J. Abergel, S. Gout, P. Ballet, J.-L. Santailler, J.-A. Nicolas, J.-P. Rostaing, S. Renet, A. Vandeneynde, L. Mathieu, and J. Le Perchec "Reaching GHz single photon detection rates with HgCdTe avalanche photodiodes detectors", Proc. SPIE 11852, International Conference on Space Optics — ICSO 2020, 118525S (2021)
[9] J. Abergel, S. Gout, A. Coquiard, L. Lechevallier, F. Berger, S. Renet, G. Lasfargues, A. Vandeneyde, S. Brunet-Manquat, G. Badanoa, A. Dumas, E. Massit, D.e Giotta, J.-L. Santailler, J. Rothman, " High operating HgCdTe APDs for free space optical communications", Presented at International Conference on Space Optics — ICSO 2022 (2022)